

Simulation of Quantum-Classical Dynamics by Surface-Hopping Trajectories

Hyojoon Kim and Raymond Kapral

ABSTRACT. Methods for simulating the dynamics of composite systems, where part of the system is treated quantum mechanically and its environment is treated classically, are discussed. Such quantum-classical systems arise in many physical contexts where certain degrees of freedom have an essential quantum character while the other degrees of freedom can be treated classically. The dynamics of these composite systems is governed by a quantum-classical Liouville equation, which is a high-dimensional matrix partial differential equation. Its solution can be obtained using hybrid Monte Carlo-Molecular Dynamics methods in terms of an ensemble of surface-hopping trajectory segments interspersed with quantum transitions. The method is illustrated by computing the rate of a nonadiabatic chemical reaction in which a two-level system is coupled to a bistable oscillator which is, in turn, coupled to a bath of harmonic oscillators.

1. Introduction

Classical molecular dynamics simulation has proven to be an extremely valuable tool for obtaining insight into physical, chemical, and biological phenomena. The greatest virtue of molecular dynamics is that the coupled Newtonian equations of motion for a large number of degrees of freedom can be solved by trajectory calculations using well-established algorithms [1, 2].

A fully quantum mechanical version of molecular dynamics for systems containing many degrees of freedom is not computationally feasible; however, in many applications, the quantum character of only small number of degrees of freedom is crucial while the dynamics of the remaining degrees of freedom can be approximated accurately by classical mechanics. A decomposition of this type is especially appropriate for a subsystem composed of light particles, such as electrons or protons, interacting with a solvent of massive molecules. This fact has motivated the construction of a quantum-classical Liouville equation description of the dynamics of such composite systems. The quantum-classical Liouville equation, when expressed in a suitable basis of quantum states, is a high-dimensional matrix partial differential equation [5, 6, 18, 19, 28].

2000 *Mathematics Subject Classification.* 60H15.

This work was supported in part by a grant from the Natural Sciences and Engineering Research Council of Canada.

Quantum (and classical) transport coefficients can be expressed in terms of time integrals of flux-flux correlation functions. Their evaluation involves sampling from suitable equilibrium initial conditions and time evolution of observables. We have shown that it is possible to compute such correlation functions by propagating observables with quantum-classical Liouville dynamics, while retaining the full quantum-mechanical equilibrium structure of system [3, 4, 8–10, 23]. In this way one can estimate quantum transport properties for a large many-body system. The calculation of the quantum equilibrium structure of a system, although a difficult problem, is far more tractable than that of the carrying out quantum time evolution. One difficulty that appears in the calculation of the quantum equilibrium structure is the fact that the statistical weight for each trajectory can be a complex number and the existence of rapidly varying phases often make sampling of initial states a challenging problem. Effective sampling algorithms are required to tackle quantum-classical systems with a large number of degrees of freedom [8, 15].

In this chapter we describe how it is possible to solve the quantum-classical Liouville equation in terms of an ensemble of classical trajectory segments interspersed by quantum transitions. The techniques we describe here are applicable to complex many-body systems and have been used to study a model proton transfer reaction in a polar molecular solvent [3]. Here, in order to illustrate the method in more a transparent context, we show how the reaction rate can be computed for a two-level system, coupled to a bistable oscillator which is, in turn, coupled to a bath of harmonic oscillators. The model captures many of the essential features of real proton transfer processes in the condensed phase, especially the coupling of the quantum protonic degree of freedom to the classical solvent polarization coordinate which, in turn, is coupled to other bath degrees of freedom.

2. Reaction Rate Constant Expressions

While the computational scheme we describe can be used to obtain a variety of transport properties, we limit our discussion here to the computation of the rate of a chemical reaction $A \rightleftharpoons B$ occurring in a many-body environment. For a quantum mechanical system in thermal equilibrium the time dependent reaction rate coefficient $k_{AB}(t)$ for this reaction may be determined from the time integral of a flux-flux correlation function [11, 27],

$$(2.1) \quad k_{AB}(t) = \int_0^t dt' \langle \hat{j}_A; \hat{j}_B(t') \rangle = \langle \hat{N}_A; \hat{N}_B(t) \rangle.$$

where $\hat{j}_A = \hat{N}_A = (i/\hbar)[\hat{H}, \hat{N}_A]$ is the flux of \hat{N}_A , with an analogous expression for \hat{j}_B , $[\cdot, \cdot]$ is the commutator and the angular brackets $\langle \hat{A}; \hat{B} \rangle = 1/\beta \int_0^\beta d\lambda \langle e^{\lambda \hat{H}} \hat{A} e^{-\lambda \hat{H}} \hat{B} \rangle$ denote a Kubo transformed correlation function, with $\beta = (k_B T)^{-1}$. The equilibrium quantum canonical average is $\langle \dots \rangle = Z_Q^{-1} \text{Tr} \dots e^{-\beta \hat{H}}$ where Z_Q is the partition function. In the reaction rate expression, $\hat{N}_{A(B)}$ is the operator that characterizes species $A(B)$. The reaction rate can be found from the plateau value of $k_{AB}(t)$.

Introducing Wigner transforms that double the phase-space dimension, the time dependent reaction rate coefficient can be written in the form [8, 9, 23]

$$(2.2) \quad k_{AB}(t) = \int d\mathcal{X} N_{BW}(\mathcal{X}, t) \bar{W}_A(\mathcal{X}, 0),$$

where the phase space variable $\mathcal{X} \equiv (\mathcal{R}, \mathcal{P})$. From this expression we see that the calculation of the reaction rate involves two aspects: how to carry out the time evolution of the observable and how to sample initial equilibrium distribution. The time evolution of the Wigner transform of the operator \hat{N}_B can be written formally as

$$(2.3) \quad \frac{d}{dt} N_{BW}(\mathcal{X}, t) = iL_W(\mathcal{X})N_{BW}(\mathcal{X}, t),$$

where iL_W is the quantum Liouville operator in Wigner-transformed form [8, 9]. The quantum equilibrium structure is described by the spectral density function W_A which is given by

$$(2.4) \quad \bar{W}_A(\mathcal{X}, 0) \equiv \frac{1}{\beta} \int_0^\beta d\lambda \int d\mathcal{X}' (iL_W(\mathcal{X}')A_W(\mathcal{X}'))W(\mathcal{X}', \mathcal{X}, i\hbar\lambda),$$

where

$$(2.5) \quad W(\mathcal{X}', \mathcal{X}, t) = \frac{1}{(2\pi\hbar)^{2\nu}Z_Q} \int d\mathcal{Z} d\mathcal{Z}' e^{-i/\hbar(\mathcal{P}\cdot\mathcal{Z} + \mathcal{P}'\cdot\mathcal{Z}')} \\ \times \left\langle \mathcal{R} + \frac{\mathcal{Z}}{2} \left| e^{-\beta\hat{H} - i/\hbar\hat{H}t} \right| \mathcal{R}' - \frac{\mathcal{Z}'}{2} \right\rangle \left\langle \mathcal{R}' + \frac{\mathcal{Z}'}{2} \left| e^{i/\hbar\hat{H}t} \right| \mathcal{R} - \frac{\mathcal{Z}}{2} \right\rangle.$$

and ν denotes the coordinate space dimension. Both the quantum dynamics and quantum equilibrium structure are difficult to compute for general systems with a large number of degrees of freedom. Below, we describe algorithms that can be used to approximately compute such quantum rate coefficient correlation functions.

3. Trajectory Description of Dynamics

3.1. Quantum-classical evolution. Since it is not computationally feasible to carry out full quantum time evolution of large many-body systems, we consider situations where the quantum system can be partitioned into two subsystems: \mathcal{S} the subsystem in whose quantum dynamics we are directly interested and its environment \mathcal{E} . We suppose that the dynamics of the environment, in the absence of coupling to \mathcal{S} , can be accurately approximated by classical equations of motion. The phase space set of coordinates \mathcal{X} can be partitioned into two sets corresponding to the \mathcal{S} and \mathcal{E} subsystems as $\mathcal{X} = (x, X)$ with $x = (r, p)$ and $X = (R, P)$. In order to obtain a representation in terms of surface-hopping dynamics, it is convenient to write the subsystem operators in the adiabatic basis. The adiabatic basis states are defined as follows: The partial Wigner transform of the Hamiltonian is $\hat{H}_W = P^2/2M + \hat{p}^2/2m + \hat{V}_W(\hat{q}, R) \equiv P^2/2M + \hat{h}_W(R)$, where $\hat{h}_W(R)$ is the Hamiltonian for the subsystem \mathcal{S} in the presence of fixed particles of the bath. The adiabatic eigenstates are the solutions of the eigenvalue problem, $\hat{h}_W(R)|\alpha; R\rangle = E_\alpha(R)|\alpha; R\rangle$ and the eigenvalues determine the Born–Oppenheimer surfaces that depend on the bath configuration. Changes of the adiabatic wavefunctions with respect to the bath coordinates lead to the breakdown of the Born–Oppenheimer approximation and give rise to transitions between different adiabatic surfaces. We term such transitions nonadiabatic effects. Using the adiabatic basis we can write

$$(3.1) \quad A_W(\mathcal{X}) = \sum_{\alpha\alpha'} \int dz e^{i/\hbar p\cdot z} \left\langle r - \frac{z}{2} \left| \alpha; R \right\rangle A_W^{\alpha\alpha'}(X) \left\langle \alpha'; R \left| r + \frac{z}{2} \right\rangle,\right.$$

where $A_W^{\alpha\alpha'}(X) = \langle \alpha; R | \hat{A}_W(X) | \alpha'; R \rangle$. Equation (2.2) can be rewritten with the operators expressed in the adiabatic basis as

$$(3.2) \quad k_{AB}(t) = \sum_{\alpha\alpha'} \int dX N_{BW}^{\alpha\alpha'}(X, t) \overline{W}_A^{\alpha'\alpha}(X, 0).$$

This expression for the quantum mechanical time dependent rate constant is exact and still intractable. We approximate it by replacing the full quantum evolution of the observable by quantum-classical Liouville evolution. In the quantum-classical limit, $N_{BW}^{\alpha'\alpha}(X, t)$ satisfies the following evolution equation, similar to (2.3) [5]:

$$(3.3) \quad \frac{d}{dt} N_{BW}^{\alpha\alpha'}(X, t) = \sum_{\beta\beta'} i\mathcal{L}_{\alpha\alpha', \beta\beta'}(X) N_{BW}^{\beta\beta'}(X, t).$$

The quantum-classical Liouville operator in the adiabatic basis $i\mathcal{L}$ is given by [5]

$$(3.4) \quad \begin{aligned} i\mathcal{L}_{\alpha\alpha', \beta\beta'}(X) &= [i\omega_{\alpha\alpha'}(R) + iL_{\alpha\alpha'}(X)]\delta_{\alpha\beta}\delta_{\alpha'\beta'} - J_{\alpha\alpha', \beta\beta'}(X) \\ &\equiv i\mathcal{L}_{\alpha\alpha'}^0(X)\delta_{\alpha\beta}\delta_{\alpha'\beta'} - J_{\alpha\alpha', \beta\beta'}(X), \end{aligned}$$

where the classical evolution operator is defined as

$$(3.5) \quad iL_{\alpha\alpha'} = \frac{P}{M} \frac{\partial}{\partial R} + \frac{1}{2} \left[F_W^\alpha(R) + F_W^{\alpha'}(R) \right] \frac{\partial}{\partial P},$$

with

$$(3.6) \quad \begin{aligned} J_{\alpha\alpha', \beta\beta'}(X) &= -\frac{P}{M} d_{\alpha\beta} \left[1 + \frac{1}{2} S_{\alpha\beta}(R) \frac{\partial}{\partial P} \right] \delta_{\alpha'\beta'} \\ &\quad - \frac{P}{M} d_{\alpha'\beta'}^* \left[1 + \frac{1}{2} S_{\alpha'\beta'}^*(R) \frac{\partial}{\partial P} \right] \delta_{\alpha\beta}. \end{aligned}$$

Here the frequency $\omega_{\alpha\alpha'}(R) \equiv [E_\alpha(R) - E_{\alpha'}(R)]/\hbar$, the Hellmann–Feynman force $F_W^\alpha = -\langle \alpha; R | \partial \hat{V}_W(\hat{q}, R) / \partial \hat{R} | \alpha; R \rangle$, the nonadiabatic coupling matrix element is $d_{\alpha\beta} = \langle \alpha; R | \nabla_R | \beta; R \rangle$, and $S_{\alpha\beta} = (E_\alpha - E_\beta) d_{\alpha\beta} [(P/M) d_{\alpha\beta}]^{-1}$ [5]. This dynamics is exact for any multi-level system bilinearly coupled to a harmonic bath and will provide a good approximation to the dynamics for general baths and couplings for systems where the bath degrees of freedom are massive compared to those of the quantum subsystem.

The formal solution of (3.3) is given by

$$(3.7) \quad N_{BW}^{\alpha\alpha'}(X, t) = \sum_{\beta\beta'} (e^{i\mathcal{L}t})_{\alpha\alpha', \beta\beta'} N_{BW}^{\beta\beta'}(X, t).$$

The propagator in each time interval satisfies the following Dyson equation [13]

$$(3.8) \quad \begin{aligned} (e^{-i\mathcal{L}t})_{\alpha\alpha', \beta\beta'} &= e^{-i\mathcal{L}_{\alpha\alpha'}^0 t} \delta_{\alpha\beta} \delta_{\alpha'\beta'} + \sum_{\nu\nu'} \int_0^t dt' e^{-i\mathcal{L}_{\alpha\alpha'}^0(t-t')} J_{\alpha\alpha', \nu\nu'}(e^{-i\mathcal{L}t})_{\nu\nu', \beta\beta'}, \end{aligned}$$

where

$$(3.9) \quad \begin{aligned} e^{-i\mathcal{L}_{\alpha\alpha'}^0(t-t')} &= e^{-i \int_t^{t'} d\tau \omega_{\alpha\alpha'}(R_{\alpha\alpha', \tau})} e^{-iL_{\alpha\alpha'}(t-t')} \\ &\equiv \mathcal{W}_{\alpha\alpha'}(t, t') e^{-iL_{\alpha\alpha'}(t-t')}, \end{aligned}$$

The terms involving the bath momentum derivative in J are difficult to evaluate exactly. In order to approximate their action on any function of the momenta, we introduce the momentum-jump approximation. In this approximation, J takes

the form of a momentum translation operator whose effect on a function of the momentum is to shift the momentum by a certain value. Using the operator identity, $(S_{\alpha\beta}/2) \cdot \partial/\partial P = \Delta E_{\alpha\beta} M \partial/(\partial(P \cdot \hat{d}_{\alpha\beta})^2)$, the action of the operator on any function $f(P)$ of the momentum may be written approximately as [5, 24]

$$\begin{aligned}
 (3.10) \quad & \left(1 + \Delta E_{\alpha\beta} M \frac{\partial}{\partial(P \cdot \hat{d}_{\alpha\beta})^2} \right) f(P) \approx e^{\Delta E_{\alpha\beta} M \partial/(\partial(P \cdot \hat{d}_{\alpha\beta})^2)} f(P) \\
 & = f(\hat{d}_{\alpha\beta}^\perp (P \cdot \hat{d}_{\alpha\beta}^\perp) + \hat{d}_{\alpha\beta} \text{sgn}(P \cdot \hat{d}_{\alpha\beta}) \sqrt{(P \cdot \hat{d}_{\alpha\beta})^2 + \Delta E_{\alpha\beta} M}) \\
 & = f(P + \hat{d}_{\alpha\beta} \Delta P),
 \end{aligned}$$

where $\Delta P = -(\hat{d}_{\alpha\beta} \cdot P) + \text{sgn}(P \cdot \hat{d}_{\alpha\beta}) \sqrt{(P \cdot \hat{d}_{\alpha\beta})^2 + \Delta E_{\alpha\beta} M}$. In the second approximate equality on the right hand side of this equation we have replaced the sum by an exponential. The momentum vector may be written in terms of its components along $\hat{d}_{\alpha\beta}$ and a perpendicular vector $\hat{d}_{\alpha\beta}^\perp$, $P = \hat{d}_{\alpha\beta} (\hat{d}_{\alpha\beta} \cdot P) + \hat{d}_{\alpha\beta}^\perp (\hat{d}_{\alpha\beta}^\perp \cdot P)$. In the last line, we used the fact that the exponential operator is a translation operator in the variable $(P \cdot \hat{d}_{\alpha\beta})^2$. Note that if there is insufficient energy in the bath to accommodate a quantum transition, the argument in the square root factor in the momentum shift will be negative. This will place a restriction on allowed transitions. Using the Dyson representation of the quantum-classical propagator in conjunction with the momentum jump approximation, Eq. (3.7) can be written as an ensemble of trajectories whose form is shown schematically in Figure 1. In this figure diagonal matrix elements of the species operator, $N_{BW}^{\alpha\alpha}$, evolve according to Newton's equations of motion on the α adiabatic surface. A quantum transition

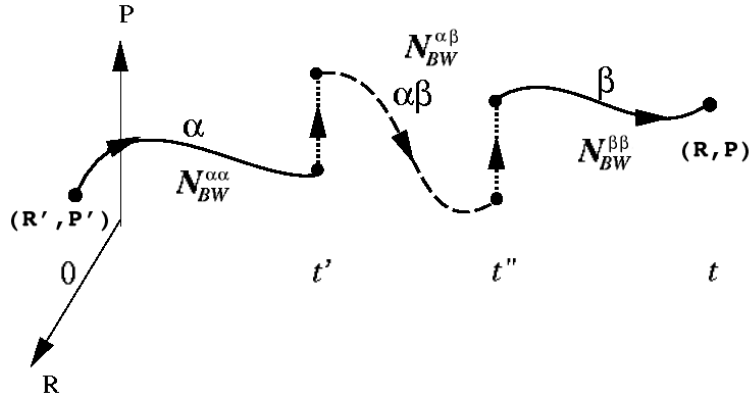


FIGURE 1. Schematic picture of a trajectory that enters into the computation of the time evolution of operator. A diagonal matrix element of the species operator $N_{BW}^{\alpha\alpha}$ evolves classically on the α adiabatic surface. The first quantum transition makes an off-diagonal matrix element of the operator $N_{BW}^{\alpha\beta}$ evolve on the mean of the α and β adiabatic surfaces with a phase factor. And the second quantum transition yields a diagonal matrix element $N_{BW}^{\beta\beta}$ on the β adiabatic surface.

gives rise to an off-diagonal matrix element of the operator, $N_{BW}^{\alpha\beta}$, and this transition is accompanied by a jump in the momentum of environment. This transition places the system in a coherent mixture of states α and β . The system evolves classically on the mean of the α and β adiabatic surfaces and a phase factor enters in the expression for the observable. A second quantum transition destroys the coherent state and yields a diagonal matrix element, $N_{BW}^{\beta\beta}$, again accompanied by a change in the momentum of the bath. Subsequent evolution takes place on the β adiabatic surface.

A similar interpretation can be given to the evolution of the density matrix. In this context we remark that the time evolution of the off-diagonal density matrix elements, integrated over bath degrees of freedom to give the quantum subsystem density matrix, is customarily used to define the decoherence time. In the above picture of the dynamics, we see from our trajectory simulation scheme that coherence is created and destroyed in passages between the diagonal and off-diagonal states. In this way, decoherence is automatically incorporated in our formalism and appears from the average over the ensemble of trajectories. In our model simulations, the average time spent in the coherent state is small compared to the typical time scale of the chemical rate process.

3.2. Simulation algorithm. The quantum-classical Liouville operator $\hat{\mathcal{L}}$ is time independent and the evolution operator can be simply decomposed into a composition of evolution operators in time segments of arbitrary length. Therefore, the evolution of a dynamical variable can be obtained by the successive application of evolution operators in small time intervals. Dividing the time interval t into N segments of lengths Δt_j such that the j th segment $\Delta t_j = t_j - t_{j-1}$, we obtain

$$(3.11) \quad (e^{i\hat{\mathcal{L}}t})_{\alpha_0\alpha'_0, \alpha_N\alpha'_N} = \sum_{(\alpha_1\alpha'_1)\cdots(\alpha_{N-1}\alpha'_{N-1})} \prod_{j=1}^N (e^{i\hat{\mathcal{L}}(t_j-t_{j-1})})_{\alpha_{j-1}\alpha'_{j-1}, \alpha_j\alpha'_j},$$

where $(\alpha_0\alpha'_0) \equiv (\alpha\alpha')$. If Δt is sufficiently small, one can make a one-point approximation to the time integral in (3.8) as

$$(3.12) \quad (e^{i\hat{\mathcal{L}}(t_j-t_{j-1})})_{\alpha_{j-1}\alpha'_{j-1}, \alpha_j\alpha'_j} \approx s e^{i\mathcal{L}_{\alpha_{j-1}\alpha'_{j-1}}^0 \Delta t} (\delta_{\alpha_j\alpha'_j, \alpha_{j-1}\alpha'_{j-1}} - \Delta t J_{\alpha_{j-1}\alpha'_{j-1}, \alpha_j\alpha'_j}) \\ = \mathcal{W}_{\alpha_{j-1}\alpha'_{j-1}}(t_{j-1}, t_j) e^{iL_{\alpha_{j-1}\alpha'_{j-1}} \Delta t} \\ \times (\delta_{\alpha_j\alpha'_j, \alpha_{j-1}\alpha'_{j-1}} - \Delta t J_{\alpha_{j-1}\alpha'_{j-1}, \alpha_j\alpha'_j}),$$

where the phase factor $\mathcal{W}_{\alpha_{j-1}\alpha'_{j-1}}(t_{j-1}, t_j) = e^{i\omega_{\alpha_{j-1}\alpha'_{j-1}}(t_j-t_{j-1})}$ associated with time segment (t_j, t_{j-1}) arises from the action of $\exp(i\mathcal{L}_{\alpha_{j-1}\alpha'_{j-1}}^0(t_j-t_{j-1}))$ on any phase space function. At the end of each segment, the system may either stay on the same energy surface or make a transition to a new state. The above expression for the propagator converges to the exact Dyson integral equation form in the limit when the number of time slices tends to infinity, the time slice interval tends to zero and the product of these two quantities is the finite total time over which the dynamics is followed [13].

The sequential short-time algorithm is easily implemented. The total time of the calculation is divided into a fixed number of time slices, the most natural choice of slice length being the molecular dynamics integration time step Δt . The phase space coordinates are propagated adiabatically in a time step and the phase factor

\mathcal{W} is computed if the evolution is on the mean of two adiabatic surfaces. The initial positions and momenta are updated from X to $X_{\Delta t}$ at time Δt by using the classical propagator $e^{iL_{\alpha_0\alpha'_0}t}$. Then, given $\alpha_0\alpha'_0$, we choose α_1 or α'_1 uniformly from the set of allowed final states. Given a choice of state, we can compute the nonadiabatic coupling matrix element d at the updated position.

At the end of each time step the probabilities [12]

$$(3.13) \quad \Pi = \theta[(P \cdot \hat{d}_{\alpha\beta})^2 + \Delta E_{\alpha\beta}M] | (P_{\Delta t}/M) \cdot d_{\alpha_0\alpha_1}(R_{\Delta t}) | \Delta t \\ \times (1 + |(P_{\Delta t}/M) \cdot d_{\alpha_0\alpha_1}(R_{\Delta t}) | \Delta t)^{-1},$$

and $1 - \Pi$, respectively, are used for acceptance or rejection of a quantum transition. In this equation the Heaviside function θ accounts for transitions that are forbidden if there is insufficient energy in the bath to cause the transition. If the transition is rejected, we have

$$(3.14) \quad N_{BW}^{\alpha_0\alpha'_0}(X, \Delta t) = \mathcal{W}_{\alpha_0\alpha'_0}(\Delta t) N_{BW}^{\alpha_0\alpha'_0}(X_{\Delta t}) \frac{1}{1 - \Pi}.$$

If the transition is accepted, we translate the momentum to $\tilde{P}_{\Delta t}$ by using the momentum-jump approximation of (3.10). We then get

$$(3.15) \quad N_{BW}^{\alpha_0\alpha'_0}(X, \Delta t) = \mathcal{W}_{\alpha_0\alpha'_0}(\Delta t) N_{BW}^{\alpha_0\alpha'_0}(R_{\Delta t}, \tilde{P}_{\Delta t}) \frac{P_{\Delta t}\Delta t}{M} \\ \cdot d_{\alpha_0\alpha_1}(R_{\Delta t}) \frac{1}{\Pi} w_{\alpha_0\alpha'_0, \alpha_1\alpha'_1},$$

where $w_{\alpha_0\alpha'_0, \alpha_1\alpha'_1}$ is an appropriate weight. This procedure may be repeated in the subsequent time slices until the N th slice is reached. By averaging the resulting quantity over initial phase space and quantum states, we can obtain the statistical average need to compute the correlation function. This will be described in more detail in the next section.

4. Sampling Equilibrium Initial States

One difference between the quantum and classical correlation function expressions for transport coefficients is that the statistical weight, which depends on the spectral density function W , can be a complex number for quantum systems. This makes sampling from quantum initial conditions difficult. For condensed phase chemical reactions occurring at high temperatures, the sampling problem is less difficult. In this limit we may write

$$(4.1) \quad \overline{W}_A(\mathcal{X}, 0) = W_A(\mathcal{X}, i\hbar\beta/2) + \mathcal{O}(\beta^2).$$

From the general expressions for the rate constant in terms of projected dynamics [7], one may show that the use of this expression in the rate constant formula is exact in the long time limit [16, 17]. This approximation will be valid if there is a large time scale separation between that for the chemical interconversion rate process and other microscopic relaxation times in the system. Although this gives rise to some differences in the short time behavior of the time-dependent rate coefficient, for long times, given reactive time scale separation, the rate coefficient extracted from the plateau value of $k_{AB}(t)$ should be given accurately. The spectral density function $W_A(\mathcal{X}, i\hbar\beta/2)$ is always real [8].

Depending on the system under investigation, it may be convenient to define the metastable states in terms of degrees of freedom of the quantum subsystem,

classical bath, or both. In order to illustrate the formalism in a simple context, we suppose that it is possible to characterize the progress of the reaction in terms of a single coordinate R_0 of the environment \mathcal{E} . For the reaction $A \rightleftharpoons B$, the A and B species operators may be defined as $\widehat{N}_{AW} = \theta(-R_0)$ and $\widehat{N}_{BW} = \theta(R_0)$ where θ is the Heaviside step function and the dividing surface has been taken to lie at $R_0 = 0$.

From the quantum-classical version of (2.5), we may perform integrations over all X' coordinates to obtain the simplified expression

$$(4.2) \quad W_A^{\alpha'\alpha} \left(X, \frac{i\hbar\beta}{2} \right) = \frac{1}{(2\pi\hbar)^\nu Z_Q} \frac{i\hbar}{M_0} \int dZ dZ'_0 \delta'(Z'_0) e^{-i/\hbar P \cdot Z} \\ \times \langle \alpha'; R_0 | \left\langle R + \frac{Z}{2} \left| e^{-\beta/2\widehat{H}} \right| - \frac{Z'_0}{2} \right\rangle \left\langle \frac{Z'_0}{2} \left| e^{-\beta/2\widehat{H}} \right| R - \frac{Z}{2} \right\rangle | \alpha; R_0 \rangle.$$

To solve this equation, we assume that the imaginary time propagator may be written in separable Hamiltonians of the subsystem and environment as $\exp(-\beta\widehat{H}) \approx \exp(-\beta\widehat{H}_{sn}) \exp(-\beta\widehat{H}_{b(n)})$ and we single out the barrier region around $R_0 = 0$ for special consideration. Separating the potential energy into a harmonic part and a remainder term, the following expression for $W_A^{\alpha\alpha}$ may be derived [8,10]

$$(4.3) \quad W_A^{\alpha\alpha} \left(X, \frac{i\hbar\beta}{2} \right) = \rho_{sn}^{\alpha\alpha}(X_0) \rho_b(X_b; R_0),$$

where

$$(4.4) \quad \rho_{sn}^{\alpha\alpha}(X_0) \\ = \frac{1}{Z_{sn}} \frac{\omega_0}{2\pi \sin 2u_0} \sqrt{\frac{2M_0 u'_0}{\pi\beta\hbar^2}} \frac{\beta P_0}{M_0 u'_0} e^{-\beta E_\alpha(R_0) - \beta/2 M_0 \omega_0^2 R_0^2 - (2M_0 u'_0)/(\beta\hbar^2) R_0^2 - \beta/(2M_0 u'_0) P_0^2},$$

and

$$(4.5) \quad \rho_b(X_b; R_0) = \frac{1}{Z_b} \prod_j \frac{\beta\omega_j}{2\pi u''_j} e^{-\beta/(u''_j) \{1/(2M_j) P_j^2 + V_{b(n)}(R_j; R_0)\}}.$$

Here M_j and ω_j are the mass and frequency for each oscillator, $u'_i \equiv u_i \cot u_i$, $u''_i = u_i \coth u_i$, and $u_i = \beta\hbar\omega_i/2$. The partition function may be also factorized as $Z_Q = Z_{sn} Z_b$. Here we have omitted the off-diagonal contribution in W_A to the rate constant since its magnitude has been shown to be very small for the values of parameters of interest [8]. Since the functions take Gaussian forms, we can easily implement sampling from the initial quantum distributions for all degrees of freedom.

The classical distribution functions can be easily obtained by taking the high temperature limits of these expressions. Using the relations $\lim_{\beta \rightarrow 0} \sqrt{a/(\pi\beta)} e^{-(a/\beta)R_0^2} = \delta(R_0)$ and $\lim_{\beta \rightarrow 0} u'_0 = \lim_{\beta \rightarrow 0} u''_j = 1$, the classical-limit expressions are given by

$$(4.6) \quad \rho_{sn}^{\alpha\alpha,cl}(X_0) = \frac{1}{Z_{sn}^{cl}} \frac{1}{2\pi\hbar} \delta(R_0) \frac{P_0}{M_0} e^{-\beta/2M_0 P_0^2 \pm \beta\Omega},$$

and

$$(4.7) \quad \rho_b^{cl}(X_b; 0) = \frac{1}{Z_b^{cl}} \prod_j \frac{\beta\omega_j}{2\pi} e^{-\beta/2M_j P_j^2 - \beta/2 M_j \omega_j^2 R_j^2}.$$

With help of these analytical expressions for W_A , we can calculate the rate constant using (3.2). The simulation results are presented in the next section.

5. Nonadiabatic Reaction Rate

As a specific example of the type of system discussed in general terms above, we consider a two-level system coupled to a quartic bistable oscillator which is in turn coupled to a heat bath of independent harmonic oscillators. The Hamiltonian operator, expressed in a diabatic basis $\{|\uparrow\rangle, |\downarrow\rangle\}$, is [21, 22]

$$(5.1) \quad \mathbf{H} = \begin{pmatrix} V_n(R_0) + \hbar\gamma_0 R_0 & -\hbar\Omega \\ -\hbar\Omega & V_n(R_0) - \hbar\gamma_0 R_0 \end{pmatrix} + \left(\frac{P_0^2}{2M_0} + \sum_{j=1}^{\nu-1} \frac{P_j^2}{2M_j} + \frac{M_j\omega_j^2}{2} \left(R_j - \frac{c_j}{M_j\omega_j^2} R_0 \right)^2 \right) \mathbf{I}.$$

The coupling to the two-level system is given by $\hbar\gamma(R_0) = -\hbar\gamma_0 R_0$. The nonlinear quartic oscillator, $V_n(R_0) = -M_0\omega_0^2 R_0^2/2 + AR_0^4/4$ is bilinearly coupled to $\nu - 1$ independent one-dimensional harmonic oscillators. The bilinear coupling is characterized by an Ohmic spectral density, $J(\omega) = \pi \sum c_j^2/(2M_j\omega_j)\delta(\omega - \omega_j)$, where $c_j = (\xi\hbar\Delta\omega M_j)^{1/2}\omega_j$, with ξ the Kondo parameter, $\omega_j = -\omega_c \ln(1 - j\Delta\omega/\omega_c)$ and $\Delta\omega = (\omega_c)/\nu - 1(1 - e^{-\omega_{\max}/\omega_c})$ with ω_c the cut-off frequency [14].

The adiabatic states are obtained by diagonalization of the two-level system Hamiltonian in (5.1) and are given by,

$$(5.2) \quad \begin{aligned} |1; R_0\rangle &= \frac{1}{\mathcal{N}}[(1 + G)|\uparrow\rangle + (1 - G)|\downarrow\rangle] \\ |2; R_0\rangle &= \frac{1}{\mathcal{N}}[-(1 - G)|\uparrow\rangle + (1 + G)|\downarrow\rangle], \end{aligned}$$

where $\mathcal{N}(R_0) = \sqrt{2(1 + G^2(R_0))}$ with $G(R_0) = \{-\Omega + \sqrt{\Omega^2 + \gamma(R_0)^2}\}/\gamma(R_0)$. The corresponding adiabatic energies are

$$(5.3) \quad E_\alpha(R) = -\frac{1}{2}M_0\omega_0^2 R_0^2 + \frac{1}{4}AR_0^4 \mp \sqrt{\Omega^2 + \gamma(R_0)^2} + V_{b(n)}(R),$$

where the sign is minus for the ground state and plus for the excited state. For the harmonic bath $V_{b(n)}(R)$ is given by $\sum_{j=1}^{\nu-1} \frac{1}{2}M_j\omega_j^2(R_j - c_j/(M_j\omega_j^2)R_0)^2$.

When γ_0 is small and the ground and excited potential surfaces are nearly parallel, the partition function for the reactant state, $n_A^{\text{eq}}Z_Q$, can be approximated by that for the mean surface and is given by

$$(5.4) \quad (n_A^{\text{eq}}Z_Q)^{-1} \approx e^{\beta V_r} \sinh(\beta\hbar\omega_r/2) \prod_{j=1} 2 \sinh(\beta\hbar\omega_j/2),$$

with ω_r the well frequency and V_r the bare potential at the bottom of the well. Using the high temperature form for (5.4) in the $t = 0+$ limit of the rate formula (3.2) we can determine the transition state theory rate constant $k_{\text{AB}}^{\text{TST}}$,

$$(5.5) \quad k_{\text{AB}}^{\text{TST}} \approx \frac{\omega_r}{2\pi} \frac{e^{\beta V_r} (e^{-\beta\Omega} + e^{\beta\Omega})}{2},$$

which will be used to scale the results presented in the figures. When the coupling between the two-level system and the quartic oscillator is negligible, the value of Ω vanishes and $k_{\text{AB}}^{\text{TST}}$ becomes the well-known value of $\omega_r e^{\beta V_r}/2\pi$. For the current symmetric oscillator, and for the parameter range under investigation, $\omega_r \approx \sqrt{2}\omega_0$.

Using these results, the transmission coefficient is given by $\kappa_{AB}(t) = k_{AB}(t)/k_{AB}^{\text{TST}}$. We label results obtained using this formula that treat the reaction coordinate and bath quantum mechanically as QRB. The limit where the reaction coordinate and bath are treated classically can be also obtained from $W_A^{\alpha\alpha}$. When this expression is used to compute the rate coefficient, we obtain the diagonal contribution to the rate obtained earlier using quantum-classical linear response theory [22]. Results obtained using this formula that treats the reaction coordinate and bath classically are labelled by CRB.

Dimensionless units with time scaled by the cut-off frequency ω_c are used in the calculations described below [22]. In particular, $t \leftarrow t\omega_c$, $R_0 \leftarrow \sqrt{M_0\omega_c/\hbar}R_0$, $\beta \leftarrow \beta\hbar\omega_c$. We set $A = 0.05$ and $\omega^\ddagger = 1$ and the bare barrier height of the $V_n(R_0)$ potential is 5 in these dimensionless units. The number of bath harmonic oscillators is $N_b = 100$ so that $\nu = 101$. We have taken $\omega_{\text{max}} = 3$. The simulation time step $dt = 0.01$.

First, we compare the QRB and CRB results for two temperatures in Figure 2. For high temperatures ($\beta = 0.1$), both the QRB and CRB results are indistinguishable, except at very short times. The CRB results for the rate constant are non-zero and equal to the transition state theory value of the rate constant at $t = 0+$ as in classical theories of the reaction rate. The QRB results for the time dependent rate constant are zero at $t = 0$, typical of quantum rate processes [7]. For the lower of the two temperatures, because of quantum effects which are included thorough initial distributions, one sees that the QRB results yield a larger rate constant than the CRB simulations. The quantum rate enhancement is similar to that seen

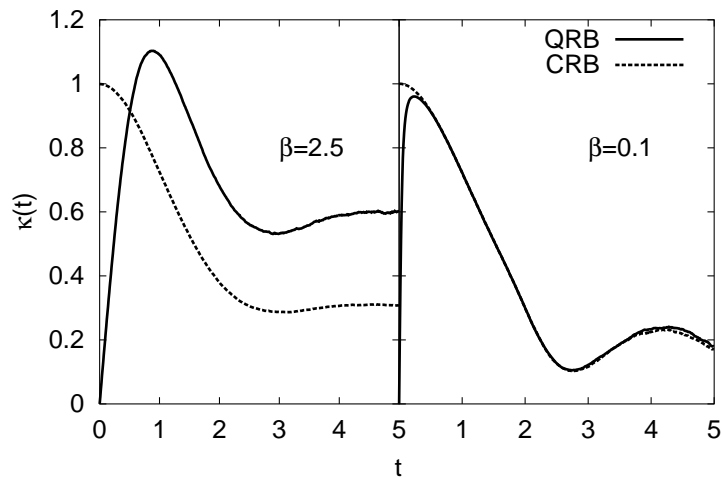


FIGURE 2. Comparison of quantum-classical nonadiabatic dynamics for cases where the equilibrium structure of the reaction coordinate and bath is treated quantum mechanically (QRB) with those where the equilibrium structure of the reaction coordinate and bath is treated classically (CRB). Parameters values: $\beta = 2.5$ (left), $\beta = 0.1$ (right), $\gamma_0 = 0.1$, $\Omega = 0.1$, and $\xi = 3$.

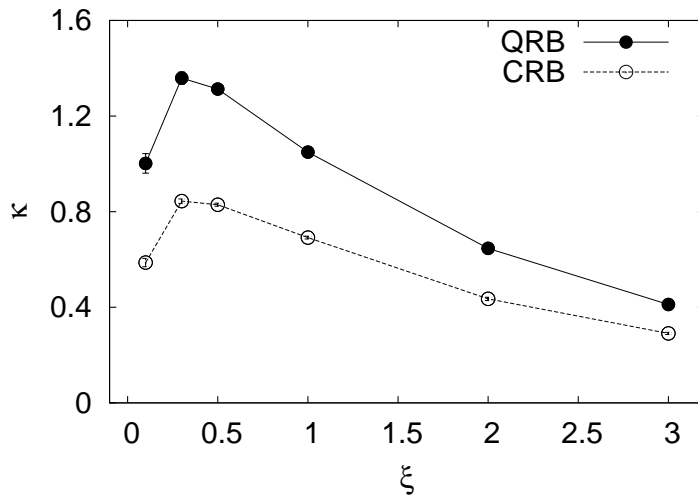


FIGURE 3. Transmission coefficient vs ξ for $\beta = 2$. The solid line denotes quantum treatments of the reaction coordinate and the bath (QRB) while the dotted line denotes classical treatments of these parts of the system (CRB).

in other studies [20, 25, 26]. Interestingly, we found that, compared to a classical description, a quantum treatment of the equilibrium structure of the reaction coordinate increases the reaction rate constant while a quantum treatment of the bath lowers the rate constant. The quantum rate enhancement is, therefore, caused by the fact that the change in the rate constant arising from quantum and classical treatments of the reaction coordinate is much greater than the corresponding change for quantum and classical treatments of the bath equilibrium structure.

In Figure 3, we plot the transmission coefficients κ_{AB}^{QRB} and κ_{AB}^{CRB} for various values of Kondo parameter ξ . Both results show similar turnover behavior for small ξ . For the model parameters used in this study, quantum effects tend to be larger for smaller values of ξ corresponding to weaker coupling to the bath modes. This trend is also consistent with the fact coupling between the reaction coordinate and the bath gives rise to decoherence and the stronger the coupling the more pronounced this effect.

6. Conclusion

The theory presented in this chapter shows how quantum chemical reaction rates of complex systems with a large number of degrees of freedom can be computed by using surface-hopping trajectories. The simulation method combines a surface-hopping dynamics derived from the quantum-classical Liouville equation with initial sampling from quantum or classical equilibrium distributions. Using this simulation scheme, the high-dimensional matrix partial differential equation that describes quantum-classical Liouville dynamics can be solved through a hybrid Monte Carlo-molecular dynamics simulation method. Future algorithmic developments in this area must focus on the construction of algorithms that are useful for arbitrarily

long times. Such developments will likely have to focus on methods for dealing with decoherence in the quantum subsystem induced by coupling to the environmental dynamics.

References

1. M.P. Allen and D.J. Tildesley, *Computer simulation of liquids*, Oxford University Press, Oxford, 1987.
2. D. Frenkel and B. Smit, *Understanding molecular simulation: from algorithms to applications*, Academic Press, San Diego, 1996.
3. G. Hanna and R. Kapral, *Quantum-classical Liouville dynamics of nonadiabatic proton transfer*, J. Chem. Phys. **122** (2005), 244505.
4. G. Hanna, H. Kim, and R. Kapral, *Quantum-classical reaction rate theory*, Quantum Dynamics of Complex Molecular Systems (D.A. Micha and I. Burghardt, eds.), Springer Ser. Chemical Phys., Springer-Verlag, Berlin, 2006, pp. 295–319.
5. R. Kapral and G. Ciccotti, *Mixed quantum-classical dynamics*, J. Chem. Phys. **110** (1999), 8919–8929.
6. ———, *A statistical mechanical theory of quantum dynamics in classical environments*, Lecture Notes in Phys., vol. 605, Springer-Verlag, Berlin, 2002, pp. 445–472.
7. R. Kapral, S. Consta, and L. McWhirter, *Chemical rate laws and rate constants*, Classical and Quantum Dynamics in Condensed Phase Simulations, Proceedings of the Internat. School of Phys. (Lerici, 1997) (B.J. Berne, G. Ciccotti, and Da.F Coker, eds.), World Scientific, Singapore, 1998, pp. 583–616.
8. H. Kim and R. Kapral, *Nonadiabatic quantum-classical reaction rates with quantum equilibrium structure*, J. Chem. Phys. **123** (2005), 194108.
9. ———, *Transport properties of quantum-classical systems*, J. Chem. Phys. **122** (2005), 214105.
10. ———, *Quantum bath effects on nonadiabatic reaction rates*, Chem. Phys. Lett. **423** (2006), 76–80.
11. R. Kubo, *Fluctuation-dissipation theorem*, Rep. Prog. Phys. **29** (1966), 255.
12. D. MacKernan, G. Ciccotti, and R. Kapral, *Surface-hopping dynamics of a spin-boson system*, J. Chem. Phys. **116** (2002), 2346–2353.
13. D. MacKernan, R. Kapral, and G. Ciccotti, *Sequential short-time propagation of quantum-classical dynamics*, J. Phys. **14** (2002), 9069–9076.
14. N. Makri, *The linear response approximation and its lowest order corrections: an influence functional approach*, J. Phys. Chem. B **103** (1999), 2823–2829.
15. N. Metropolis, A.W. Rosenbluth, M.N. Rosenbluth, A.H. Teller, and E. Teller, *Equation of state calculations by fast computing machines*, J. Chem. Phys. **21** (1953), 1087–1092.
16. W.H. Miller, *Quantum-mechanical transition-state theory and a new semiclassical model for reaction-rate constants*, J. Chem. Phys. **61** (1974), 1823–1834.
17. W.H. Miller, S.D. Schwartz, and J.W. Tromp, *Quantum-mechanical rate constants for bimolecular reactions*, J. Chem. Phys. **79** (1983), 4889–4898.
18. S. Nielsen, R. Kapral, and G. Ciccotti, *Non-adiabatic dynamics in mixed quantum-classical systems*, J. Stat. Phys. **101** (2000), 225–242.
19. ———, *Statistical mechanics of quantum-classical systems*, J. Chem. Phys. **115** (2001), 5805–5815.
20. E. Rabani, G. Krilov, and B.J. Berne, *Quantum mechanical canonical rate theory: a new approach based on the reactive flux and numerical analytic continuation methods*, J. Chem. Phys. **112** (2000), 2605–2614.
21. A. Sergi and R. Kapral, *Nonadiabatic reaction rates for dissipative quantum-classical systems*, J. Chem. Phys. **119** (2003), 12776–12783.
22. ———, *Quantum-classical dynamics of nonadiabatic chemical reactions*, J. Chem. Phys. **118** (2003), 8566–8575.
23. ———, *Quantum-classical limit of quantum correlation functions*, J. Chem. Phys. **121** (2004), 7565–7576.
24. A. Sergi, D. MacKernan, G. Ciccotti, and R. Kapral, *Simulating quantum dynamics in classical environments*, Theor. Chem. Accts. **110** (2003), 49–58.

25. M. Topaler and N. Makri, *Quantum rates for a double-well coupled to a dissipative bath — accurate path-integral results and comparison with approximate theories*, J. Chem. Phys. **101** (1994), 7500–7519.
26. H.B. Wang, X. Sun, and W.H. Miller, *Semiclassical approximations for the calculation of thermal rate constants for chemical reactions in complex molecular systems*, J. Chem. Phys. **108** (1998), 9726–9736.
27. T. Yamamoto, *Quantum statistical mechanical theory of the rate of exchange chemical reactions in the gas phase*, J. Chem. Phys. **33** (1960), 281–289.
28. C. Zhu, A.W. Jasper, and D.G. Truhlar, *Non-Born–Oppenheimer Liouville–von Neumann dynamics. evolution of a subsystem controlled by linear and population-driven decay of mixing with decoherent and coherent switching*, J. Chem. Theory Comput. **1** (2005), 527–540.

DEPARTMENT OF CHEMISTRY, UNIVERSITY OF TORONTO, TORONTO, ONTARIO M5S 3H6,
CANADA.

E-mail address: hkim@chem.utoronto.ca

E-mail address: rkapral@chem.utoronto.ca